An Algorithm for Non-invasive Mapping Based on Cardiac Anatomy and 12-lead Electrocardiogram Data

Svyatoslav Khamzin[1], Anastasia Bazhutina[1], Alexandr Sinitca[1], Mikhail Chmelevsky[1,2,3], Stepan Zubarev[1,2], Margarita Budanova[1,2], Werner Rainer[1]

[1]XSpline S.p.A, Bolzano, Italy
[2]Almazov National Medical Research Centre, Saint-Petersburg, Russia
[3]Division of Cardiology, Fondazione Cardiocentro Ticino, Lugano, Switzerland

Abstract

Cardiac mapping provides detailed insights into a patient's unique heart anatomy and electrical patterns. In this paper, we propose an algorithm that integrates cardiac anatomical information with 12-lead electrocardiogram (ECG) data to create activation maps without invasive procedures. To find the activation map of the corresponding ECG of the patient, we solve the multiple forward ECG problems. We use the anisotropic eikonal equation in conjunction with the Lead-Field approach to compute the ECG. By varying the activation area parameters and conductivity parameters in the eikonal equation we generate a subset of ECGs. We use a variational autoencoder to parameterise the 12-channel ECG. Then we train a surrogate model on the generated dataset and apply it to find the closest solutions to the clinical ECG. To calculate the activation map, we use the average solution obtained from the found range of parameters that give close solutions to the patient's ECG. Electroanatomical mapping (EAM) data from the left ventricular endocardium of five patients were used to validate the algorithm. Comparing local activation times, the mean absolute error was 16 ms and a mean correlation of 0.82 was obtained between EAM endocardial activation times and the proposed algorithm.

1. Introduction

The use of electrocardiography (ECG) in conjunction with medical imaging data such as computed tomography (CT) or magnetic resonance imaging has the potential to solve the problem of reconstructing electrical activity on the surface of the heart, also known as non-invasive mapping. In recent years, many efforts have been made to solve this problem using electrocardiographic imaging (ECGi) [1]. However, recent studies [2] show that in some cases this approach inaccurately reproduces the electrical activation map and demonstrates low correlation between invasive and non-invasive electrical activation patterns.

Another prominent approach non-invasive reconstruction of electrical activity is to use an electrophysiological model to identify optimal model parameters that reproduce the patient's ECG. This approach shows promising results on artificial [3,4] and invasive dataset [5]. In this study we propose a new algorithm of non-invasive mapping based on electrophysiological modelling which we validate on invasive dataset.

2. Methods

2.1. Data

This study utilized retrospective data from five patients with a wide QRS complex (>120 ms) and presumed left bundle branch block. These data include cardiac CT images, 12-lead ECG recordings and electroanatomical mapping (EAM) recordings of the left ventricular endocardial surface. For each patient, a 3D patient-specific geometry model of the heart, torso and lungs was created by a medical expert using semi-automated segmentation of the cardiac CT scans. Each invasive dataset contains between 116 and 354 numbers of recorded electrogram (EGM) signals.

2.2. Data processing

To process the EGM signals we are used the CoM algorithm described in [6]. In addition, we relied on this article [7] to evaluate the quality of the original signals. Thus, we processed all the EGM signals in the dataset. We then compared the obtained local activation times (LAT) with those originally recorded. The mean correlation of local activation times processed by the internal algorithms of the EAM system with those processed by the algorithm described above was 0.91 for the left ventricular endocardium.

Gaussian process regression was used to interpolate the LAT's on the surface of the heart with an error estimate in the form of a standard deviation given for each point. This type of interpolation was based on the article [7], where the author proposed an algorithm to evaluate the error of the EAM data from the distance between the EAM points to the surface mesh and the fragmentation of the electrogram signals at specific points.

A finite element tetrahedral mesh was then generated using Gmsh package [8]. In the next step, the universal ventricular coordinate (UVC) system was defined at each node of the heart geometry [9]. To accurately represent the anisotropic properties of the cardiac tissue, a rule-based method [10] was employed to assign myocardial fiber orientation. The coordinates of the ECG leads were placed on the torso surfaces by a medical expert for further calculation of the 12-lead ECG.

2.3. ECG processing

In a first step, we estimated the boundaries of the QRS complex in the patients' ECG signals using the Hamilton-Thompson algorithm [11]. Then to parameterize the ECG signals we used a neural network. To standardise the inputs for the neural network, we cut off the signal with the QRS complex within the boundaries.

We used a convolutional variation autoencoder (CVAE) to convert the ECG signal into a set of features (also called latent space). The input to this neural network was a QRS signal of dimension (i,300,12), where i is the number of 12-lead QRS signals to be processed. CVAE has three system units: encoder, latent space unit and decoder. An encoder consists of several successive convolutional blocks. Each block consists of a convolution layer, a batch normalisation layer, an activation layer and a maximum pooling layer. The encoder block transforms a QRS complex into k feature vectors, where k is the parameter of the encoder. We used the same encoder unit for the QRS signal of each lead with shared weights. At the output of the encoder, the received features are concatenated into a block of latent space and the dimension is further reduced by the linear transformation. One-dimensional deconvolution blocks are used to decode the signal. Each block consists of a convolutional transpose layer, a batch normalisation layer, and an activation layer.

The loss function for training this neural network is as follows:

$$L = \sum_{n=1}^{12} ||QRS_{true} - QRS_{pred}||^2 + KL[N(\mu, \sigma), N(0, 1)] \tag{1}$$

, where QRS_{true} is input QRS signal in one on the 12 lead, QRS_{pred} - decoded QRS signal, KL - Kullback-Leibler divergence, $N(\mu, \sigma)$ - normal distribution with parameters μ and σ given out from latent space.

2.4. Electrophysiology model

To model the depolarisation process of the heart, we used the eikonal approach. In the eikonal equation, the arrival times of the wave front t_a in the myocardial area Ω are described based on the spatially inhomogeneous orthotropic velocity function, encoded as $D(x)$, and the certain initial activation area Γ at time t_0. The eikonal equation has the form:

$$\begin{cases} \sqrt{\nabla t_a^T \mathbf{D} \nabla t_a} = 1 & \text{in } \Omega \\ t_a = t_0 & \text{in } \Gamma \end{cases} \tag{2}$$

where t_a is a positive function describing the wavefront arrival time at location x and D symmetric positive definite 3×3 tensor which is determined by the myocardial fiber direction field and myocardial tissue conductivity along:across set here as 6.5:1.

To calculate the 12-lead ECG, the lead-field approach is used, which is written as follows:

$$V(t) = \int_{\Omega} \nabla Z(x) \cdot G_i \nabla V_m(x, t) dx \tag{3}$$

where Ω is the heart domain and $Z(x)$ is the lead field of the specific ECG lead. The lead field is the potential field created by a unit current applied at the electrode location x_i:

$$\nabla \cdot (G \nabla Z(x) = \sum c_i \delta(x - x_i) \tag{4}$$

where c_i are relative contributions of the two or more electrodes and δ is Dirac's delta function.

2.5. Model parameter setup

To simulate the His-Purkinje system, we used the approach proposed in the [4] based on myocardial activation from root points. These root points characterise the junctions of Purkinje fibres with the myocardium. In order to limit the range of parameters that need to be varied when using the model, we restricted the range of variation of root points coordinates using UVC in accordance with experimental data of the human His-Purkinje system anatomy [12].

Additionally, to implement possible heterogeneity of myocardial conduction properties (e.g. caused by the presence of fibrosis) we restricted the range of possible conduction velocities of the excitation wave across the myocardium from 0.2 m/s to 0.7 m/s. For the variation of conduction velocities, we used an interpolation function with conduction parameters defined at the centres of the segments. To interpolate the value to the other mesh nodes, we used Gaussian processes regression.

2.6. Surrogate model

To decrease the quantity of simulations, we employed a "surrogate" model that translates the varying model parameters into a vector of CVAE features. We employed a neural network comprising dense blocks that include dense, batch normalization, and dropout layers. Mean square error was selected as the loss function to train the neural network.

2.7. Inference of activation maps

For inference of electrophysiological model parameters related to patient's ECG we used features obtained from CVAE. We solve the following optimisation problem:

$$f(p) = (CVAE(QRS_{pat}) - SM(p))^2 \qquad (5)$$

where f is function for optimization, $CVAE(QRS_{pat})$ is CVAE features obtained from patient's QRS, $SM(p)$ is CVAE features predicted by surrogate model for the variable parameters of the electrophysiological model p.

We solve the problem for 100 different initial parameter vectors to obtain sets of parameters reproducing the real ECG. Then using the mean values of the obtained solutions we reproduce the activation map.

2.8. Validation metrics

We used three different metrics to validate our results. The first one is the correlation coefficient between LAT on the LV endocardial surfaces (EAM vs non-invasive). To do so, we use the Spearman correlation coefficient.

As a second validation metric we used the mean absolute error (MAE) between endocardial activation times (EAM vs non-invasive). It can be calculated using the following formula:

$$\mathrm{MAE} = \frac{1}{\mathrm{n}} \sum_{\mathrm{i}=1}^{\mathrm{n}} \left| \mathrm{Y_i} - \widehat{\mathrm{Y_i}} \right| \qquad (6)$$

where n is the number of points and Y_i and $\widehat{Y_i}$ are LAT values.

The last metric is related to the quantification of the distance between the two late activation points determined invasively and non-invasively. To remove any artifacts resulting from noise in the invasive data, we calculate the centre of mass of the points contained in the surface region with the 15% of latest activation, for both invasive and non-invasive activation maps, and then calculate the Euclidean distance between the centres of mass.

3. Results

We present here a comparison of proposed non-invasive algorithm activation maps and EAM data. In table 1 shown results of computed validation metrics for non-invasive activation maps. In all cases, the Pearson correlation between EAM and non-invasive algorithm was more then 0.75 and mean correlation was 0.82. Figure 1 shows an example of activation maps obtained from EAM data and the non-invasive algorithm.

On the other hand, it is worth noting that the average distance error was 14.9 mm, which is a significant error. However, the average distance from the EAM points to the cardiac mesh was about 9.2 $\pm$ 6.1 mm. Therefore, we assume that the obtained error characterises not only the accuracy of the algorithm, but also includes the error obtained in the process of invasive data collection and transfer of these data to the anatomical surface obtained from CT images. The mean error in the comparison local activation times between the non-invasive activation map and the EAM data was 16 $\pm$ 9.1 ms. We compare this value with the standard deviation obtained by the Gaussian process interpolation algorithm described in [7]. Obtained standard deviation ranged from 3.5 to 12.1 ms.

Table 1. Comparison metrics for validation dataset and algorithm results.

Patient number	LAT correlation	MAE, ms	Distance error, mm	ECG correlation
001	0.76	21.5 $\pm$ 13.9	21.3	0.85
002	0.84	12.8 $\pm$ 6.7	8.6	0.91
003	0.85	11.5 $\pm$ 6.4	19.0	0.90
004	0.79	23.3 $\pm$ 12.2	21.5	0.85
005	0.88	11.7 $\pm$ 7.4	4.1	0.92
Mean	0.82	16.1 $\pm$ 9.1	14.9	0.89

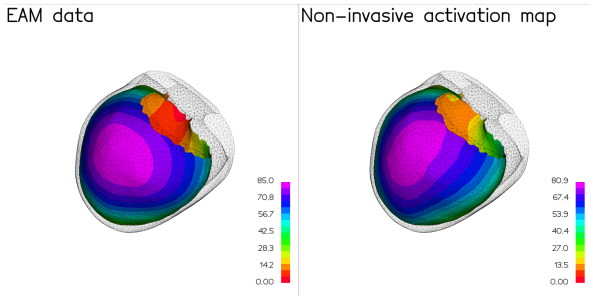

Figure 1. Example of comparison activation times measured invasively (left panel) and computed using 12-lead ECG by non-invasive algorithm.

A 0.89 correlation coefficient was obtained when computed and clinical ECGs were compared. An example

of comparison of ECG signals is shown in Figure 2.

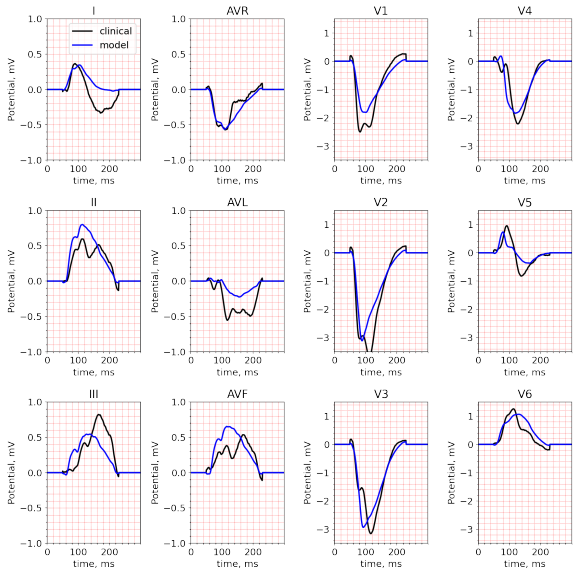

Figure 2. Example of comparison clinical and obtained by non-invasive algorithm ECGs.

4. Conclusion

In this paper we proposed a new algorithm for non-invasive cardiac mapping. Our algorithm shows a high correlation between the patient's 12-lead ECGs and calculated ECG, with a correlation of 0.89. Comparing endocardial local activation times obtained by proposed algorithm with EAM data from five patients, non-invasive algorithm showed a mean correlation of 0.82 between left ventricular endocardial maps. The MAE for local activation times was 16 ms and the mean absolute error between late activation zones was 14.9 mm. These results demonstrate the potential of a non-invasive mapping system to estimate the electrical activity of the heart.

References

[1] Pereira H, Niederer S, Rinaldi CA. Electrocardiographic imaging for cardiac arrhythmias and resynchronization therapy. Europace 10 2020;22:1447. ISSN 15322092.

[2] Duchateau J, Sacher F, Pambrun T, Derval N, Chamorro-Servent J, Denis A, Ploux S, Hocini M, Jaïs P, Bernus O, et al. Performance and limitations of noninvasive cardiac activation mapping. Heart rhythm 2019;16(3):435–442.

[3] Pezzuto S, Perdikaris P, Costabal FS. Learning cardiac activation maps from 12-lead ecg with multi-fidelity bayesian optimization on manifolds. IFAC PapersOnLine 1 2022;55:175–180. ISSN 2405-8963.

[4] Camps J, Lawson B, Drovandi C, Minchole A, Wang ZJ, Grau V, Burrage K, Rodriguez B. Inference of ventricular activation properties from non-invasive electrocardiography. Medical Image Analysis 10 2021; 73:102143. ISSN 1361-8415.

[5] Pezzuto S, Prinzen FW, Potse M, Maffessanti F, Regoli F, Caputo ML, Conte G, Krause R, Auricchio A. Reconstruction of three-dimensional biventricular activation based on the 12-lead electrocardiogram via patient-specific modelling. EP Europace 4 2021; 23:640–647. ISSN 1099-5129.

[6] El Haddad M, Houben R, Stroobandt R, Van Heuverswyn F, Tavernier R, Duytschaever M. Novel algorithmic methods in mapping of atrial and ventricular tachycardia. Circulation Arrhythmia and Electrophysiology 2014;7(3):463–472.

[7] Coveney S, Corrado C, Roney CH, Wilkinson RD, Oakley JE, Lindgren F, Williams SE, O'Neill MD, Niederer SA, Clayton RH. Probabilistic interpolation of uncertain local activation times on human atrial manifolds. IEEE Transactions on Biomedical Engineering 2019; 67(1):99–109.

[8] Geuzaine C, Remacle JF. Gmsh: a three-dimensional finite element mesh generator with built-in pre-and post-processing facilities. In Proceedings of the Second Workshop on Grid Generation for Numerical Computations, Tetrahedron II. 2007; .

[9] Bayer J, Prassl AJ, Pashaei A, Gomez JF, Frontera A, Neic A, Plank G, Vigmond EJ. Universal ventricular coordinates: A generic framework for describing position within the heart and transferring data. Medical Image Analysis apr 2018;45:83–93. ISSN 13618423.

[10] Bayer JD, Blake RC, Plank G, Trayanova NA. A novel rule-based algorithm for assigning myocardial fiber orientation to computational heart models. Annals of Biomedical Engineering oct 2012;40(10):2243–2254. ISSN 00906964.

[11] Arzeno NM, Deng ZD, Poon CS. Analysis of first-derivative based qrs detection algorithms. IEEE Transactions on Biomedical Engineering 2 2008; 55:478–484. ISSN 00189294.

[12] Choquet C, Boulgakoff L, Kelly RG, Miquerol L. New insights into the development and morphogenesis of the cardiac purkinje fiber network: Linking architecture and function. Journal of Cardiovascular Development and Disease 2021 Vol 8 Page 95 8 2021;8:95. ISSN 2308-3425.

Address for correspondence:

Svyatoslav Khamzin
39100 Via Josef Ressel 2F, Bolzano, Italy
khamzin@xspline.com